Available online at www.sciencedirect.com

ScienceDirect

Procedia Computer Science 184 (2021) 258–265

Procedia Computer Science

www.elsevier.com/locate/procedia

The 12th International Conference on Ambient Systems, Networks and Technologies (ANT)
March 23 - 26, 2021, Warsaw, Poland

STS-EPR: Modelling individual mobility considering the spatial, temporal, and social dimensions together

Giuliano Cornacchia[a,b,*], Luca Pappalardo[b]

[a]*Department of Computer Science, University of Pisa, Pisa, Italy*
[b]*Institute of Information Science and Technologies (ISTI), National Research Council of Italy (CNR), Pisa, Italy*

Abstract

Modelling human mobility is crucial in several scientific areas, from urban planning to epidemic modeling, traffic forecasting, and what-if analysis. On the one hand, existing models focus on the spatial and temporal dimensions of mobility only, while the social dimension is often neglected. On other hand, models that embed a social mechanism have trivial or unrealistic spatial and temporal mechanisms. We propose STS-EPR, a mechanistic model that captures the spatial, temporal, and social dimensions of human mobility together. Our results show that STS-EPR generates realistic trajectories, making it better than models that lack either in the social, the spatial, or the temporal mechanisms. STS-EPR is a step towards the design of mechanistic models that can capture all the aspects of human mobility in a comprehensive way.

Keywords: human mobility; generative models; synthetic trajectories; social network; data science; mechanistic models

1. Introduction

Mobility data are crucial in different contexts, such as computational epidemiology, traffic forecasting, urban planning, what-if analysis, ride-sharing simulations, and the design of protocols for ad hoc and opportunistic networks [3, 8, 10, 14, 19, 7, 21]. Unfortunately, privacy implications restrict sharing mobility datasets because they contain sensitive information about the individuals whose movements are described [12, 11, 17, 18]. A way to overcome this issue is to design generative mobility models [10, 3], i.e., algorithms that generate synthetic trajectories that reproduce human mobility patterns.

Most individual models focus on capturing the spatial patterns, such as the power-law distribution in jump lengths and characteristic distances [4, 8] and the tendency to return to locations visited before [8]. For example, the Ex-

* Corresponding author: Giuliano Cornacchia
E-mail address: giuliano.cornacchia@phd.unipi.it

1877-0509
10.1016/j.procs.2021.03.035

ploration and Preferential Return model (EPR) [20] is based on two competing mechanisms: *exploration*, a random walk process with truncated power-law jump length distribution; and *preferential return*, which reproduces humans' propensity to return to previously visited locations. Among the mechanistic models that improve EPR by adding increasingly sophisticated mechanisms [13, 2, 1], TimeGeo [9] and DITRAS [14] embed a temporal mechanism that captures the circadian propensity to travel. The social dimension of human mobility is often neglected in EPR-like models, although about 10-30% of human movements has social purposes [5]. As an exception, GeoSim [22] use an individual preference and social influence mechanism, but its spatial and temporal realism is limited. Another strand of works focus on design multidimensional agent environment models that consider the social dimension of individuals [6, 7].

In this paper, we propose STS-EPR (Spatial, Temporal, and Social EPR), a model that combines: *(i)* a mechanism that takes into account the spatial distance between locations and their collective relevance [19, 16]; *(ii)* a temporal mechanism to capture the individuals' tendency to follow a circadian rhythm [14]; *(iii)* a mechanism that models the social dimension of human mobility [22]; *(iv)* an action-correction mechanism that deals with borderline cases during the simulation. We conduct experiments using check-ins of thousands of users in three cities worldwide and show that STS-EPR's trajectories are realistic with respect to several spatial, temporal, and social aspects of mobility.

Open source. The link to the open data and the code to reproduce our models and experiments is available at: https://github.com/kdd-lab/2019_Cornacchia. An implementation of STS-EPR, GeoSim and DITRAS is also available in library scikit-mobility (https://github.com/scikit-mobility/scikit-mobility) [15].

2. The STS-EPR model

We define a mobility trajectory as a sequence $T = \langle (r_1, t_1), \ldots, (r_n, t_n) \rangle$ where t_i is a timestamp ($\forall i \in [1, n); t_i < t_{i+1}$) and $r_i = (x_i, y_i)$ where x_i and y_i are coordinates on a bi-dimensional space [10]. We assume that agents move on a spatial tessellation L, representing a bi-dimensional space's tiling, resulting in a non-overlapped set of locations. Every location has a weight corresponding to its collective relevance and as a representative point the tile's centroid expressed as a pair of coordinates: $L = \langle (r_1, w_1), \ldots, (r_n, w_n) \rangle$ where w_j is the weight of the tile j and r_j its representative point. We represent an agent's a visitation pattern as a location vector lv_a of $|L|$ locations. The vector's *j-th* element, $lv_a[j]$, contains the number of times a visited r_j. We assume that an agent's network of contacts G influences their movements. $G = (V, E)$ is a graph where V is the set of agents and E the social ties between them.

STS-EPR takes as input the number N of synthetic agents, the spatial tessellation L, the undirected graph G, a mobility diary generator MDG, and the time interval of the simulation. The model outputs N synthetic trajectories. STS-EPR consists of four phases: initialization, action selection, location selection, and action-correction (Figure 1). After the initialization phase, the agents execute the action selection, the location selection, and the action-correction phases until a stopping criterion is satisfied (e.g., the number of hours to simulate is reached).

Initialization. Each edge's weight in G indicates the mobility similarity of the linked agents (the cosine similarity of their location vectors). The weights are initialized to 0 and updated during the simulation. The model assigns to each agent a mobility diary produced by MDG. In STS-EPR, the MDG considered is a Markov Model that captures the individuals' probability to follow or break their routine at specific times of the day, exploiting the conditional probability of real trajectory data [14]. A mobility diary MD for an agent a is defined as $\mathrm{MD}_a = \langle (ab_0, t_1), (ab_1, t_2), \ldots (ab_j, t_{j+1}), (ab_0, t_{j+2}), (ab_1, t_{j+3}) \ldots) \rangle$, where ab is an abstract location, ab_0 denotes a's starting location, t_i is a timestamp. The probability $p(r_i)$ for an agent of being assigned to a starting physical location $r_i \in L$ is $\propto w_i$, where w_i is the location's relevance. Each agent moves according to its own mobility diary's entries at the time specified. If the current abstract location is ab_0, the agent visits the starting location; otherwise, ab_i is converted into a physical one through the following steps.

Action selection. When moving, an agent can select between two competing mechanisms: exploration and preferential return. Exploration models the decreasing tendency to explore new locations over time [19]. Preferential return reproduces individuals' propensity to return to locations they explored before [19]. An agent explores a new location with probability $P_{exp} = \rho S^{-\gamma}$, or returns to a previously visited one with a complementary probability $P_{ret} = 1 - \rho S^{-\gamma}$, where S is the agent's number of unique visited locations and $\rho = 0.6$, $\gamma = 0.21$ are constants [19]. At that point, the agent determines whether or not the location's choice will be affected by the other agents, selecting between the

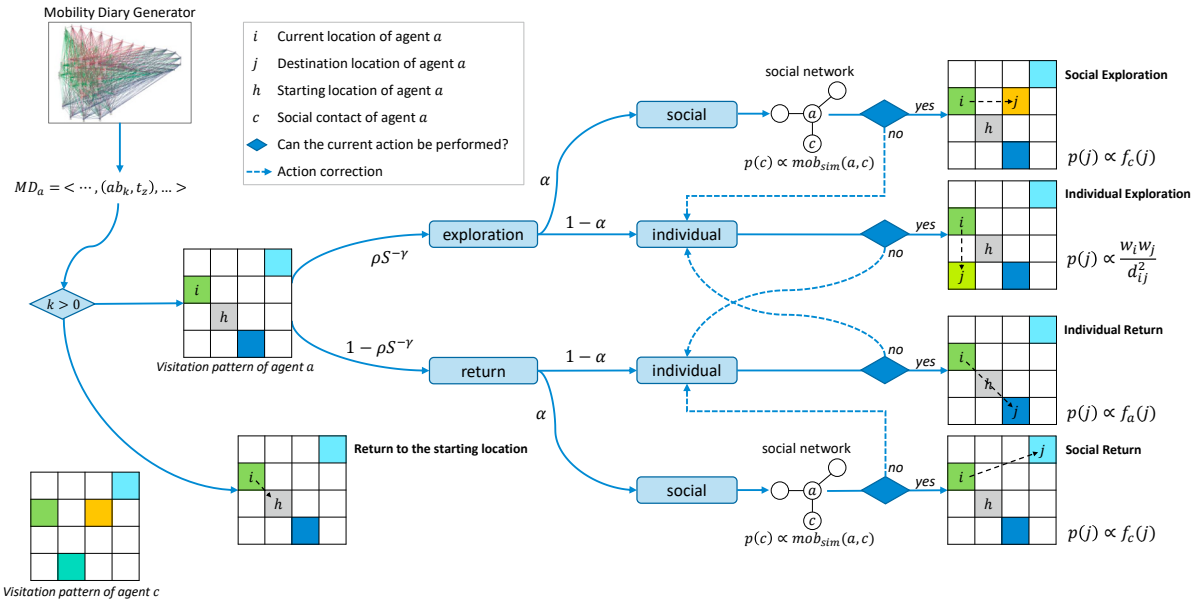

Fig. 1. Schematic description of STS-EPR. An individual moves according to the entry in its mobility diary. If the abstract location in the diary is ab_0, then the individual returns to its starting location; otherwise it decides whether to explore a new location or return to a previously visited one. At that point, the agent determines whether or not its social contacts affect its choice for the location to visit next. If the selected action cannot be performed, it is corrected with an executable one (dashed arrows indicate action corrections).

individual and the social influence mechanisms. With a probability $\alpha = 0.2$, the agent's social contacts influence its movement [22]. With a complementary probability of $1 - \alpha$, the agent's choice is not influenced by the other agents.

Location selection. At this point, the agent decides which location will be the destination of its next displacement. The sets of locations an agent a can visit or return to are $exp_a = \{i \mid lv_a[i] = 0\}$ and $ret_a = \{i \mid lv_a[i] > 0 \wedge i \notin \{s_a, c_a\}\}$, respectively, where s_a and c_a are the indices of the starting and current location of agent a. The set of the location visited, without the constraints of the current and starting location, is $vis_a = \{i \mid lv_a[i] > 0\}$. The visitation frequency of a to a location r_i is: $f_a(r_i) = \frac{lv_a[i]}{\sum_{j=1}^{|L|} lv_a[j]}$.

- **Individual Exploration:** a chooses a new location to explore from exp_a. Individuals are more likely to move at small rather than long distances but also take into account the location's collective relevance [14]. We use the gravity law to couple distance and relevance [13]. If a is currently at location r_j, during the Individual Exploration action selects an unvisited location r_i, with $i \in exp_a$, with probability $p(r_i) \propto \frac{w_i w_j}{d_{ij}^2}$, where d_{ij} is the distance between locations r_i and r_j with relevances w_i, w_j.
- **Social Exploration:** a selects an agent c among its social contacts in G. The probability $p(c)$ for c to be selected is proportional to the mobility-similarity between them: $p(c) \propto mob_{sim}(a, c)$. After the contact c is chosen, the candidate location to explore is an unvisited location for a that was visited by c, i.e., the location is selected from set $A = exp_a \cap vis_c$; the probability $p(r_i)$ for a location r_i, with $i \in A$, to be selected is proportional to the visitation pattern of c, namely $p(r_i) \propto f_c(r_i)$.
- **Individual Return:** a picks the return location from the set ret_a with a probability proportional to its visitation pattern. The probability for a location r_i with $i \in ret_a$ to be chosen is: $p(r_i) \propto f_a(r_i)$.
- **Social Return:** c is selected as in the Social Exploration action, and the location a returns to is picked from the set $A = ret_a \cap vis_c$. The probability $p(r_i)$ for a location r_i to be selected is proportional to the visitation pattern of the agent c, namely $p(r_i) \propto f_c(r_i)$.

Action correction. The set of possible locations an agent can reach is limited. For example, it may happen that the agent visited all locations at least once and there are no locations to explore. To comply with these constraints, we include an action-correction phase, executed if the location selection phase does not allow movements in any location.

- **No location in social choices**: If an agent a decides to move with the influence of a social contact c but $ret_a \cap vis_c = \varnothing$ or $exp_a \cap vis_c = \varnothing$ (no locations visited by both c and a or no locations visited by c and unvisited by a), we execute an individual action preserving a's choice to explore or return.
- **No new location to explore**: When an agent a decides to explore but it visited all the locations at least once ($exp_a = \varnothing$), we force the agent to make an Individual Return.
- **No return location**: If an agent a, currently at location r_i, decides to perform an Individual Return, and r_i is the only location visited so far (besides the starting location), it cannot return to any location ($ret_a = \varnothing$). We force a to make an Individual Exploration.

3. Experiments

3.1. Datasets

Mobility. We use a public LBSN (Location-Based Social Network) dataset D_{FS}, collected by Yang et al. [23], which includes a set of global-scale checkins gathered from the social network platform Foursquare over 22 months (from April 2012 to January 2014). A checkin describes a user's real-time position with its social contacts. From D_{FS}, we extract three datasets that describe the mobility of individuals in New York City, London, and Tokyo, from the 10th of April 2012 to the 10th of July 2012. Table 1 reports the statistics of the three datasets.

Social graphs. D_{FS} is associated with a snapshot of a social network G_{FS}, antecedent at the collection period, that describes the social relationships between individuals (i.e., mutual follow on Twitter) in D_{FS}. We associate each of the three datasets with a social graph, extracted from G_{FS}, which describes the social links among the Foursquare users.

3.2. Experimental settings

We simulate the mobility of agents moving for three months in New York City, London, and Tokyo, using STS-EPR and two state-of-the-art models: GeoSim [22] and DITRAS [14]. GeoSim embeds a social mechanism but has trivial spatial and temporal mechanisms; DITRAS has sophisticated spatial and temporal mechanisms but does not embed a social mechanism. For each combination of city and model, we run a trajectory generation for five times and take, for each standard mobility measure (see Section 3.3), the average and standard deviation of the Kullback-Leibler divergence between the distribution of that measure on the set of generated trajectories and the set of real trajectories in that city. We discretize the physical space using a squared tessellation of 300 meters.[1]

3.3. Mobility measures

We evaluate the models' realism with respect to the distribution of the following standard mobility measures [10, 3]:

- Jump Length Δr, the distance between two consecutive locations visited by an individual [8];
- Radius of Gyration r_g, the typical distance traveled by an individual during the period of observation [8, 16];
- Visits per Location V_l, the relevance of a location described as its attractiveness at a collective level;
- Location Frequency $f(r_i)$, the probability of visiting a location r_i [8];
- Waiting Time Δt, the elapsed time between two consecutive visited locations;
- Entropy E_{unc}, the predictability of the movements of an individual u [20];
- Activity per Hour $t(h)$, the number of movements made by the individuals at every hour of the day [14, 9];

[1] The squared tessellation is performed using python library scikit-mobility [15].

Table 1. A summary of the properties of the three datasets and the corresponding social graphs extracted from the public Foursquare dataset D_{FS} and the social graph G_{FS}, respectively.

City	# checkins	# users	# edges	average degree
London	14,895	622	1,185	3.81
New York City	37,489	1,001	1,755	3.506
Tokyo	231,471	4,396	18,183	8.272

- Mobility Similarity mob_{sim}, the cosine-similarity of two individuals' location vectors [22, 5, 23];

We quantify the similarity between each measure's distributions for real and synthetic trajectories using the Kullback–Leibler divergence (KL).

4. Results

Our results highlight the importance of coupling both distance and relevance in the location selection phase to obtain realistic trajectories regarding the spatial measures (Table 2). Concerning Δr and r_g, STS-EPR is more realistic than GeoSim, which cannot reproduce neither the Δr distribution (Figures 2(a), 3(a) and 4(a)) nor the r_g distribution. STS-EPR is also slightly more realistic than DITRAS concerning Δr, except for New York City (Table 2). DITRAS is the best model regarding the distribution of r_g; STS-EPR fails in reproduce correctly the distribution for small radii with the exception of Tokyo, where DITRAS and STS-EPR achieve similar KL scores (0.2417 and 0.2504, respectively). GeoSim generates trajectories with the most realistic distribution of $f(r_i)$ but fails in reproducing accuratly the V_l distribution (Figures 2(d), 3(d) and 4(d)). STS-EPR is more realistic than DITRAS on $f(r_i)$, and for V_l the KL scores of STS-EPR are 58.62% (New York City), 27.73% (London), and 79.47% (Tokyo) better than DITRAS. None of the models can replicate the distribution of E_{unc}, though the best one is this sense is STS-EPR.

The temporal measures, Δt and $t(h)$ (Figures 2(f), 3(f) and 4(f)), are better reproduced by STS-EPR and DITRAS, since they use the same temporal mechanism (MDG). The small fluctuations of the scores obtained from these two models are caused only by the pseudo-random nature of each execution. Although GeoSim can reproduce the Δt distribution, it fails in reproducing $t(h)$ because its trajectories that do not follow the circadian rhythm of individuals.

As for the distribution of the social measure mob_{sim}, STS-EPR reproduces it better than GeoSim and DITRAS, especially for Tokyo (KL=0.014, Table 2), presumably because the social graph of users in Tokyo is the largest in terms of nodes and edges, giving a more realistic representation of the individuals' sociality. STS-EPR can capture the distribution's shape better than GeoSim; the latter can reproduce correctly the distribution only for values ≤ 0.25 (Figures 2(h), 3(h) and 4(h)). DITRAS is not able to capture the mobility similarity as it does not include a mechanism that models the sociality between agents.

The results for New York City, London, and Tokyo (Table 2) are consistent, suggesting that STS-EPR do not depend on the specific characteristics of the geographic area, i.e., STS-EPR is geographically transferable.

5. Discussion

Coupling spatial distance and location relevance is crucial to improve the realism for spatial measures such as jump length, radius of gyration, and location relevance. Indeed GeoSim, which does not use the gravity law, cannot capture the shape of these distributions. Although STS-EPR and DITRAS use the same spatial mechanisms, STS-EPR approximates better the distribution of number of visits per location, while DITRAS reproduces accurately the distribution of the radius of gyration also for small radii. The use of the mobility diary generator is crucial to capture the temporal patterns of human mobility as it allows reproducing both the waiting time and the propensity to move at specific times during the day. The combination of realistic social and temporal mechanisms allows STS-EPR to reproduce the mobility similarity in the most realistic way. Although GeoSim embeds a social mechanism, its generated trajectories are unrealistic with respect to the social measure, and so are those generated by DITRAS, which does not embed any social mechanism.

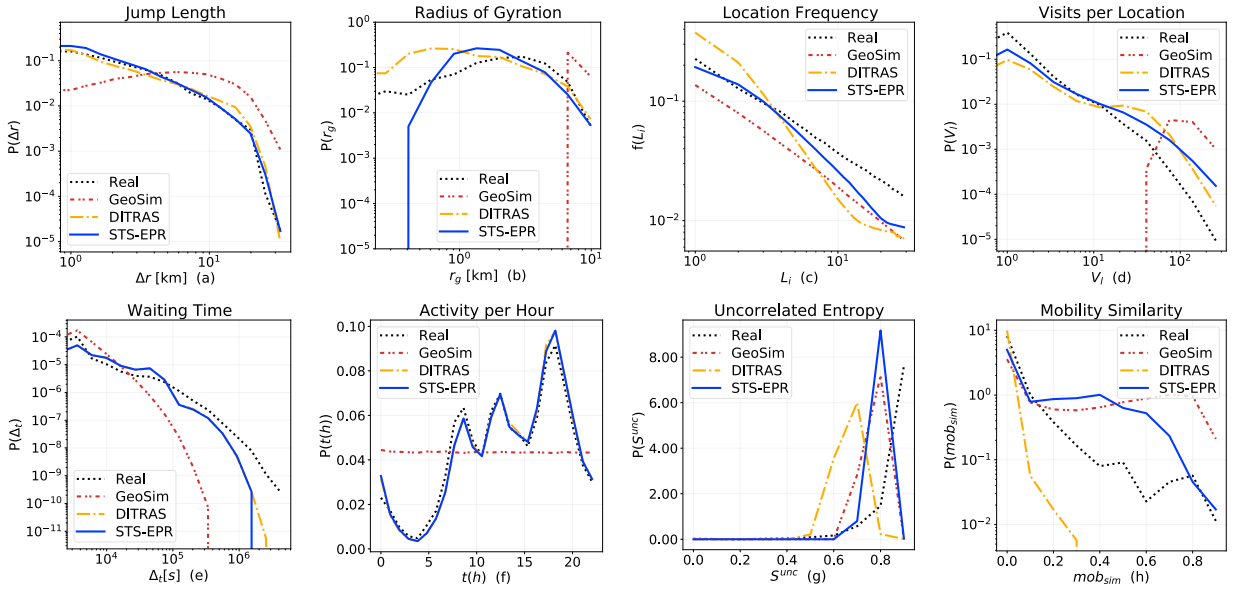

Fig. 2. Distribution of jump length (a), radius of gyration (b), location frequency (c), visits per location (d), waiting time (e), activity per hour (f), uncorrelated entropy (g), and mobility similarity (h) of real data (black dotted line) and data generated by GeoSim (red dash-dotted line), DITRAS (orange dash-dotted line), and STS-EPR (blue line), for New York City.

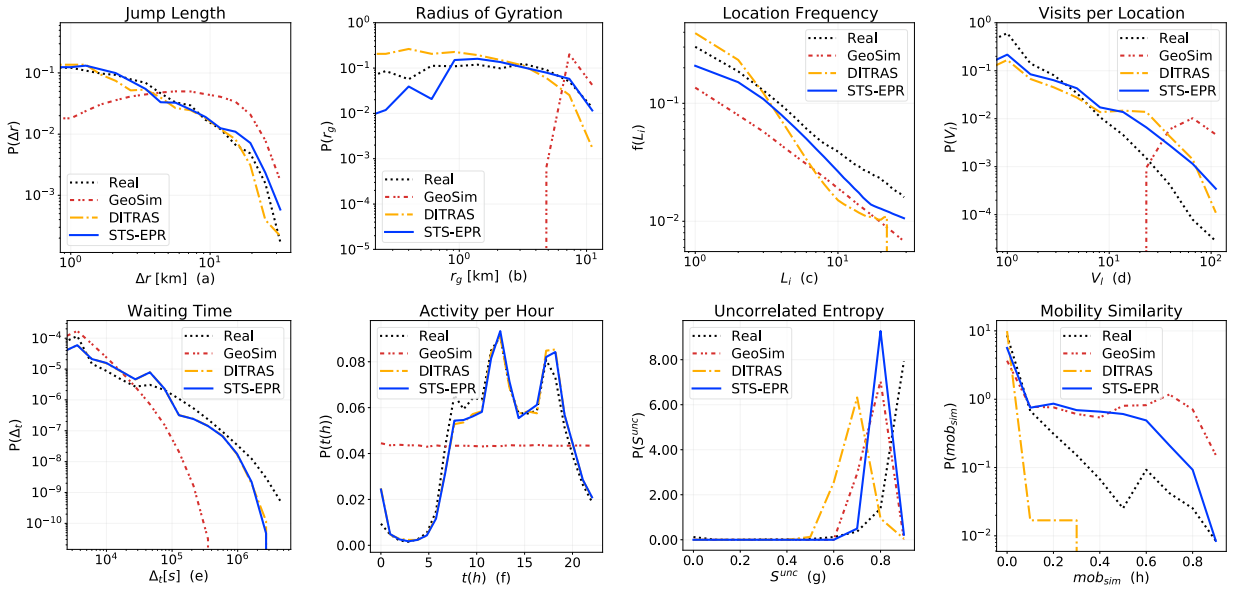

Fig. 3. Distribution of jump length (a), radius of gyration (b), location frequency (c), visits per location (d), waiting time (e), activity per hour (f), uncorrelated entropy (g), and mobility similarity (h) of real data (black dotted line) and data generated by GeoSim (red dash-dotted line), DITRAS (orange dash-dotted line), and STS-EPR (blue line), for London.

It is worth noting that the inclusion of the social dimension in STS-EPR help improve the realism concerning both the spatial and temporal measures. This result highlights the importance of sociality: though often neglected in generative mobility models, it is essential to model properly individual human mobility.

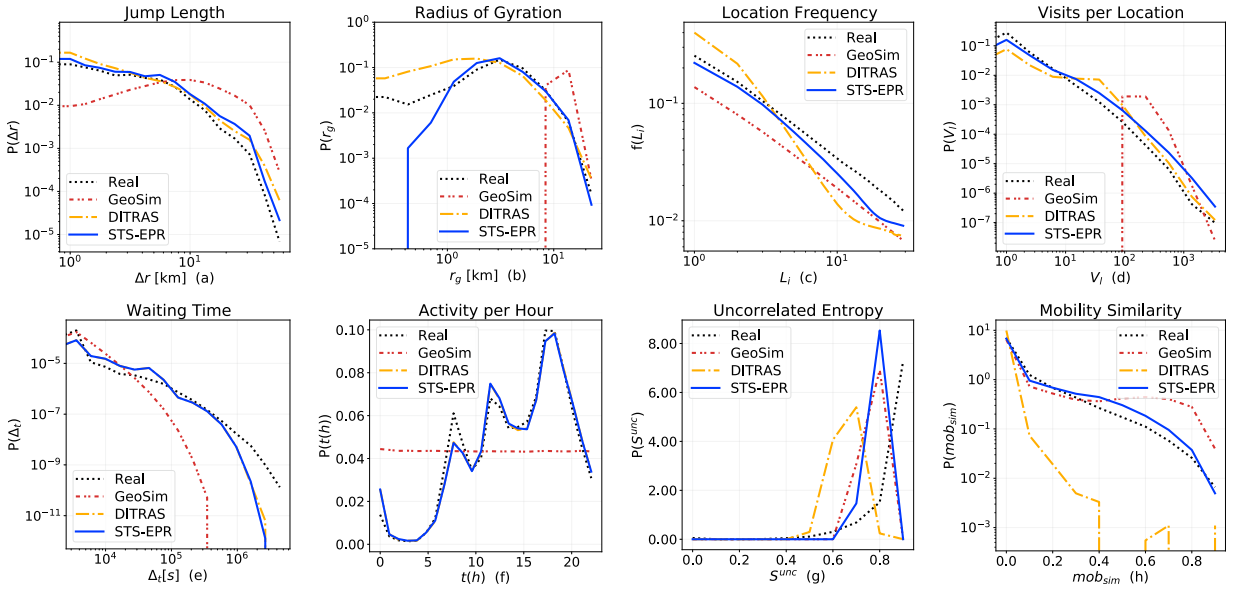

Fig. 4. Distribution of jump length (a), radius of gyration (b), location frequency (c), visits per location (d), waiting time (e), activity per hour (f), uncorrelated entropy (g), and mobility similarity (h) of real data (black dotted line) and data generated by GeoSim (red dash-dotted line), DITRAS (orange dash-dotted line), and STS-EPR (blue line), for Tokyo.

Table 2. Results for London, Tokyo and New York City. For each measure, we show the average and the standard deviation of the KL divergence. The best results for a combination of city and measure are highlighted in bold.

	Model	Δr	r_g	$f(r_i)$	Vl	Δ_t	$t(h)$	E_{unc}	mob_{sim}
London	GeoSim	0.5036 ±0.0075	4.9381 ±0.0932	**0.0016 ±0.0001**	4.427 ±0.0069	0.1962 ±0.0043	0.281 ±0.0003	8.5182 ±0.0003	0.6097 ±0.0079
	DITRAS	0.0221 ±0.0022	**0.1813 ±0.0239**	0.1094 ±0.0	0.1428 ±0.006	0.166 ±0.0031	0.0119 ±0.0004	3.8816 ±0.1897	0.4347 ±0.0516
	STS-EPR	**0.0108 ±0.0016**	0.4609 ±0.233	0.0097 ±0.0003	**0.1032 ±0.0126**	**0.1626 ±0.0035**	**0.0116 ±0.001**	**2.6749 ±0.1169**	**0.2543 ±0.01**
Tokyo	GeoSim	0.7257 ±0.002	4.8165 ±0.0042	**0.0002 ±0.0**	3.0957 ±0.0148	0.2354 ±0.0003	0.2837 ±0.0006	7.1242 ±0.0593	0.0931 ±0.0017
	DITRAS	0.0628 ±0.0025	**0.2417 ±0.0171**	0.1409 ±0.0	0.1101 ±0.0048	0.2007 ±0.003	**0.0074 ±0.0001**	5.0034 ±0.2708	0.923 ±0.0375
	STS-EPR	**0.0485 ±0.0013**	0.2504 ±0.0746	0.0108 ±0.0002	**0.0226 ±0.0019**	**0.2001 ±0.0024**	0.0076 ±0.0001	**4.8717 ±0.2247**	**0.014 ±0.0009**
New York City	GeoSim	0.5947 ±0.0062	5.3913 ±0.0051	**0.0071 ±0.0004**	3.6418 ±0.0069	0.1973 ±0.0004	0.18 ±0.0005	8.0483 ±0.0579	0.5879 ±0.0149
	DITRAS	**0.0091 ±0.0006**	**0.2987 ±0.0359**	0.193 ±0.0026	0.1281 ±0.0044	**0.1665 ±0.0032**	**0.0066 ±0.0003**	**4.8881 ±0.0248**	0.5425 ±0.038
	STS-EPR	0.0188 ±0.0015	0.3886 ±0.0284	0.0318 ±0.0008	**0.0531 ±0.004**	0.1705 ±0.0047	0.0071 ±0.0005	5.028 ±1.1511	**0.3066 ±0.0044**

6. Conclusion

We proposed a mechanistic generative model that considers the spatial, temporal, and social dimensions together during the generation of the synthetic mobility trajectories. Our results showed that the modelling all the three dimensions at the same time produces more realistic trajectories than existing models that lack either the social, the spatial, or the temporal mechanisms. STS-EPR can be particularly useful to computational epidemiology, in which agent-based simulations of human movements may help decision making for the containment of epidemics.

An opportunity for future improvement consists of embedding deep learning techniques (e.g., Generative Adversarial Networks and Variational Autoencoders) to model aspects of mobility that are not captured by the current mechanisms [10]. In the meantime, our model is a step towards the design of a mechanistic model that can capture all the aspects of human mobility in a complete way.

Acknowledgements. This work has been supported by project H2020 SoBigData++ grant agreement 871042.

References

[1] Alessandretti, L., Sapiezynski, P., Lehmann, S., Baronchelli, A., 2018. Evidence for a conserved quantity in human mobility. Nature Human Behaviour 2. doi:10.1038/s41562-018-0364-x.
[2] Barbosa, H., de Lima-Neto, F.B., Evsukoff, A., Menezes, R., 2015. The effect of recency to human mobility. EPJ Data Science 4, 21. URL: https://doi.org/10.1140/epjds/s13688-015-0059-8, doi:10.1140/epjds/s13688-015-0059-8.
[3] Barbosa-Filho, H., Barthelemy, M., Ghoshal, G., James, C., Lenormand, M., Louail, T., Menezes, R., Ramasco, J.J., Simini, F., Tomasini, M., 2018. Human mobility: Models and applications. Physics Reports 734, 1–74.
[4] Brockmann, D., Hufnagel, L., Geisel, T., 2006. The scaling laws of human travel. Nature 439, 462–5. doi:10.1038/nature04292.
[5] Cho, E., Myers, S., Leskovec, J., 2011. Friendship and mobility: User movement in location-based social networks, pp. 1082–1090.
[6] Galland, S., Balbo, F., Gaud, N., Rodriguez, S., Picard, G., 2015. Contextualize agent interactions by combining social and physical dimensions in the environment.
[7] Galland, S., Knapen, L., Yasar, A.U.H., Gaud, N., Janssens, D., Lamotte, O., Koukam, A., Wets, G., 2014. Multi-agent simulation of individual mobility behavior in carpooling. Transportation Research Part C: Emerging Technologies 45. doi:10.1016/j.trc.2013.12.012.
[8] Gonzalez, M.C., Hidalgo, C., Barabasi, A.L., 2008. Understanding individual human mobility patterns. Nature 453, 779–82.
[9] Jiang, S., Yang, Y., Gupta, S., Veneziano, D., Athavale, S., Gonzalez, M.C., 2016. The timegeo modeling framework for urban mobility without travel surveys. Proceedings of the National Academy of Sciences 113, 201524261. doi:10.1073/pnas.1524261113.
[10] Luca, M., Barlacchi, G., Lepri, B., Pappalardo, L., 2020. Deep learning for human mobility: a survey on data and models. arXiv:2012.02825.
[11] Montjoye, Y.A., Gambs, S., Blondel, V., Canright, G., Cordes, N., Deletaille, S., Engø-Monsen, K., García-Herranz, M., Kendall, J., Kerry, C., Krings, G., Letouzé, E., Luengo-Oroz, M., Oliver, N., Rocher, L., Rutherford, A., Smoreda, Z., Steele, J., Wetter, E., Bengtsson, L., 2018. On the privacy-conscientious use of mobile phone data. Scientific Data 5, 180286. doi:10.1038/sdata.2018.286.
[12] Montjoye, Y.A., Hidalgo, C., Verleysen, M., Blondel, V., 2013. Unique in the crowd: The privacy bounds of human mobility. Scientific reports 3, 1376. doi:10.1038/srep01376.
[13] Pappalardo, L., Rinzivillo, S., Simini, F., 2016. Human mobility modelling: Exploration and preferential return meet the gravity model. Procedia Computer Science 83. doi:10.1016/j.procs.2016.04.188.
[14] Pappalardo, L., Simini, F., 2017. Data-driven generation of spatio-temporal routines in human mobility. Data Mining and Knowledge Discovery 32. doi:10.1007/s10618-017-0548-4.
[15] Pappalardo, L., Simini, F., Barlacchi, G., Pellungrini, R., 2020. scikit-mobility: a python library for the analysis, generation and risk assessment of mobility data. arXiv:1907.07062.
[16] Pappalardo, L., Simini, F., Rinzivillo, S., Pedreschi, D., Giannotti, F., Barabasi, A.L., 2015. Returners and explorers dichotomy in human mobility. Nature Communications 6. doi:10.1038/ncomms9166.
[17] Pellungrini, R., Pappalardo, L., Pratesi, F., Monreale, A., 2017. A data mining approach to assess privacy risk in human mobility data. ACM Trans. Intell. Syst. Technol. 9. URL: https://doi.org/10.1145/3106774, doi:10.1145/3106774.
[18] Pellungrini, R., Pappalardo, L., Simini, F., Monreale, A., 2020. Modeling adversarial behavior against mobility data privacy. IEEE Transactions on Intelligent Transportation Systems , 1–14.
[19] Song, C., Koren, T., Wang, P., Barabasi, A.L., 2010a. Modelling the scaling properties of human mobility. Nature Physics 6.
[20] Song, C., Qu, Z., Blumm, N., Barabasi, A.L., 2010b. Limits of predictability in human mobility. Science (New York, N.Y.) 327, 1018–21.
[21] Tomasini, M., Mahmood, B., Zambonelli, F., Brayner, A., Menezes, R., 2017. On the effect of human mobility to the design of metropolitan mobile opportunistic networks of sensors. Pervasive and Mobile Computing 38, 215 – 232.
[22] Toole, J., Herrera-Yague, C., Schneider, C., Gonzalez, M.C., 2015. Coupling human mobility and social ties. Journal of the Royal Society, Interface / the Royal Society 12. doi:10.1098/rsif.2014.1128.
[23] Yang, D., Qu, B., Yang, J., Cudre-Mauroux, P., 2019. Revisiting user mobility and social relationships in lbsns: A hypergraph embedding approach, pp. 2147–2157. doi:10.1145/3308558.3313635.